WARSAW UNIVERSITY OF TECHNOLOGY Index 351733
FACULTY OF CIVIL ENGINEERING
COMMITTEE FOR CIVIL AND WATER ENGINEERING
POLISH ACADEMY OF SCIENCES ISSN 1230-2945

DOI: 10.24425/ace.2022.141890

ARCHIVES OF CIVIL ENGINEERING

Vol. LXVIII ISSUE 3 2022

pp. 353 –368

Research paper

Computer modelling of point supported laminated glass panes

Piotr Woźniczka[1]

Abstract: In recent years significant progress has been made in structural application of glass elements in building industry. However, the issues related to computer modelling of glass panes, as well as analytical procedures allowing for taking into account the bonding action of PVB foil are not widely known in the engineering environment. In this paper results of numerical study of laminated glass plates are presented. The scope of the research covers over 40 cases of panes. Narrow (characterized by edge length $ab > 2$) and square ($a/b = 1$) panes made of two or three layer laminated glass have been taken into account. The paper deals mainly with point supported glass. However, selected results for linearly supported plates have been included as well for comparison. For each considered case an advanced computational model have been developed within the environment of Abaqus software. Pointwise supports have been modelled using methods of various complexity. The obtained results have been compared with the results of standard calculations using Wölfel–Bennison and Galuppi–Royer–Carfagni hypotheses. The analytical procedures proposed by CEN have been applied as well. As a result, recommendations for static calculations of laminated glass panes have been formulated. The computational procedure based on the hypothesis presented by L. Galuppi and G. Royer-Carfagni should be considered the most universal. The remaining methods may be applied only in limited scope. In order to estimate maximum principal stress in the support zone an advanced computer model has to be used. The support may be modelled in an exact or simplified manner.

Keywords: computer modelling, laminated glass, nonlinear analysis, point support, thin plate theory

[1]PhD., Eng., Cracow University of Technology, Faculty of Civil Engineering, Warszawska 24, 31-155 Cracow, Poland, e-mail: pwozniczka@pk.edu.pl, ORCID: 0000-0002-5471-9526

1. Introduction

Contemporary laminated glass is made using PVB foil as the bonding layer between the glass panes (cf. [1–3]). Simplified modelling of elements of this type in the first phase allows for neglecting the influence of bonding action exerted by the foil [4–6]. Thus it is assumed that individual glass panes may freely slide with respect to one another. However, more recent research shows (for instance [7–9]), that the bonding layers, in spite of stretching and creep, exhibit significant bonding action. Effectiveness of this action depends on material properties of the PVB layer. The shear modulus G_F of the bonding layer is a measure of the susceptibility to rheological phenomena. The values of this modulus may be determined using equations [10], depending on the duration of load application and ambient temperature, or using material data supplied by the manufacturer of the PVB foil [11, 12].

Static calculations of glass panes made of laminated glass use the standard procedures applicable to monolithic thin plates exhibiting large deflections. The influence of rheological phenomena is taken into account by replacing the actual plate thicknesses with effective values. The effective values are derived by application of hypotheses assuming curvature compatibility between the layered element comprising of n layers and exhibiting stiffness EJ_{full} and a quasi-monolithic element exhibiting stiffness EJ_{eff}. In European codification the computational procedures according to the Wölfel–Bennison hypothesis [13, 14], or alternative procedures according to the hypothesis developed by L. Galuppi and G. Royer-Carfagni [15–17] are applied to this purpose. The exact solutions, derived based on rheological models, have been obtained for bar elements consisting of two or three layers [3, 7, 8]. Other possible computational approaches and analytical solutions are presented in [18–20], while results of experimental research is described in e.g. [21]. Finally, the extensive review of available standard recommendations for point supported laminated glass is discussed in [7].

The results of computer simulations for monolithic panes and panes made of laminated glass, using abovementioned computational procedures, have been presented in the paper [11]. However, the cases considered in that paper dealt mainly with linearly supported panes. In current paper the point supported laminated glass panes, important from the practical point of view, are considered in detail. Narrow (characterized by edge length ratio $a/b > 2$) and square ($a/b = 1$) panes made of two or three layer laminated glass have been considered. For each case an advanced computational model had been developed within the environment of Abaqus software [22]. The obtained results have been compared with the results of standard calculations using Wölfel–Bennison (denoted below as W–B) and Galuppi–Royer–Carfagni (denoted below as G–R–C) hypotheses. The analytical procedures proposed by CEN/TC 250 N 1060 [7] (denoted below as CEN) have been applied as well. Selected results determined for linearly supported panes have been included as well for comparison.

2. Methods

Static analysis conforming to the W–B, G–R–C and CEN computational procedures for the case of narrow plate ($a/b > 2$) has been conducted on the structural example of glass steps. The following assumptions have been made regarding the analysed component:

- glass steps dimensions in plan 350×1500 mm,
- service category B according to the code EN 1991-1-1 (variable load $p_k = 3.0$ kN/m^2),
- destruction consequence class CC2,
- load application time for the service load 10 years, the ambient temperature of $T = 25°$C in an air conditioned room,
- disc dimensions in the case of point support have been assumed as for element depicted in Fig. 1.

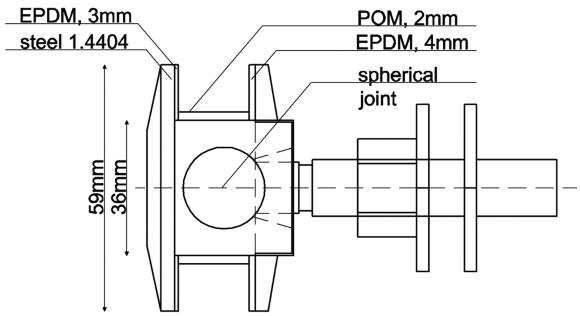

Fig. 1. Pointwise support

Two variants of glass steps made of tempered glass bonded by SafleX foil [12] have been considered: variant 1 – two layers of glass of combined thickness 2×10 mm +0.76 mm = 20.76 mm and variant 2 – three layers of glass of combined thickness 8 + 6 + 8 mm $+2 \times 0.76$ mm = 23.52 mm. Depending on the analysed case a linear articulated or point articulated support has been assumed. In each case dead weight of the plate itself has been accounted for during calculations.

At the subsequent stage comparative calculations have been conducted for square panes of edge length $a = b$. The case of a pane having dimensions 1.5×1.5 m linearly or point supported has been considered. The distance between point supports was 1.3×1.3 m. The remaining assumptions have been the same as for narrow plates.

In the case of advanced computer simulations the Abaqus software [22] has been applied. The real geometry of the glass panes, including PVB foil, has been replicated during calculations. In selected cases, in order to accurately render boundary conditions, an exact geometry of the rotule system support has been assumed. The components made of glass have been modelled using C3D20R brick finite elements ($3 \times 3 \times 3$ Gauss stations), while hybrid C3D8H elements have been applied to model the components made of materials exhibiting high value of Poisson's ratio. The $20 \times 20 \times 10$ mm, $15 \times 15 \times 10$ mm and $10 \times 10 \times 10$ mm finite elements have been used, while for selected cases a convergence test consisting in decreasing the element size to $5 \times 5 \times 5$ mm has been executed. The results

convergent to the results of initial model had been obtained, therefore it has been assumed that no additional increase in finite element mesh density is required. It has to be underlined, however, that the guidelines contained in [15] indicate the necessity to apply a finer finite element mesh. According to these guidelines, at least two finite elements should be used along the thickness of glass plate and at least four finite elements along the thickness of PVB foil. Introduction of a so dense subdivision, even for a plate of limited size is very computationally "costly", and therefore impossible in many practical cases. In the zones adjacent to point supports a finer finite element mesh has been applied each time.

Geometrically nonlinear model has been applied during calculations. The load has been applied in five increments, in a manner analogous to [11]. In the computer models where the geometry of supports has been recreated full bonding has been assumed between elements. Only for the contact surface between EPDM and glass plate a two surface contact problem has been defined. Friction and separation in the normal direction after contact have been accounted for. Hyperelastic material model (Marlow form) with material data assumed according to the technical specifications given by certain manufacturer has been applied to model the behaviour of the EPDM washer. It has to be underlined, that this is a simplified approach. In reality the strain-stress relationship for EPDM materials highly depends on the strain rate [23,24]. In the remaining cases a classical linear elastic model has been used. The rheological phenomena have been accounted for by application of reduced shear modulus value G_F for bonding layer (according to the data given in [12]). Basic characteristics of applied materials are listed in the Table 1.

Table 1. Properties of the materials

Material	Young's modulus [MPa]	Poisson's ratio	Density [kg/m^3]
tempered glass	70 000	0.22	2500
PVB	1.476	0.476	1080
EPDM	6	0.4999	~1050
POM	3 000	0.44	~1420
steel 1.4404	200 000	0.30	8000

Finally, for pointwise supports an alternative computational approach has been tested. The document [15] presents a simplified way of computer modelling the support zone. In the proposed method it is assumed that the rotule is not exactly rendered, but is replaced by an area support of identical diameter. At the same time no indications had been given regarding the estimation of the stiffness of this substitute support. The stresses at the edge of the opening are determined by multiplying the stresses obtained from the computer model by an appropriate magnifying coefficient. One may determine the value of this stress concentration factor using formulae (2.1) to (2.3) [25].

$$K_t = 3 - 0.947\sqrt{\frac{d}{h}} + 0.192\left(\frac{d}{h}\right), \quad \text{simple bending } (M_1 = M, M_2 = 0) \tag{2.1}$$

$$K_t = 2.7 - 0.647\sqrt{\frac{d}{h}} + 0.129\left(\frac{d}{h}\right), \tag{2.2}$$

$$\text{cylindrical bending } (M_1 = M, \quad M_2 = \nu M), \quad \frac{d}{h} \leq 7.0$$

$$K_t = 2.0, \quad \text{isotropic bending } (M_1 = M_2 = M) \tag{2.3}$$

where: K_t – stress concentration factor, d – hole diameter, h – plate thickness, M_1, M_2 – bending moments in both directions, $\nu = 0.3$.

According to the recommendations [15] calculation methods based on the effective glass pane thickness may not be used to analyse the support zone. In practice this means, that the computer simulations using volumetric finite elements have to be applied. Under such circumstances the issue of ignoring the actual opening diameter while using the abovementioned stress concentration factor seems to be too far reaching and unnecessary simplification. The alternative approaches to determine the stresses in the support zone with necessary parameters are given among others in [7, 26, 27] and [28].

In the case of W–B and G–R–C procedures, an engineering software AxisVM [29] has been applied. The effective thickness of the glass pane determined during calculations has been entered into the computer model each time. In the considered cases shell finite elements and geometrically nonlinear analysis have been applied. The verification of the applicability of AxisVM software with respect to the structures made of laminated and monolithic glass has been discussed in [11]. Other computer codes can be used as well [30].

The adopted detailed structural solutions require additional discussion. Firstly, in engineering practice an application of the "planar system" elements is possible instead of supports depicted in Fig. 1. The differences between these two systems have been schematically presented in [15]. Stress distributions in the support zone would vary, depending on the assumed point support solution. The "planar system" elements have been analysed, among others, in [26]. Secondly, the codes [31] and [32] contain additional structural recommendations pertaining to point supported glass panes and panes subject to pedestrian traffic. According to these codes the minimum support diameter should be 50 mm. In addition, the distance between the support and the plate edge should be not smaller than 80 mm. Finally, the PVB foil should be at least 1.52 mm (2×0.76 mm) thick. In the examples considered here the support diameter has been assumed to be 59 mm, while the distance from the edge was 100 mm. However, for comparative purposes it has been decided to apply only a single layer of PVB foil 0.76 mm thick.

3. Results

The considered cases have been prepared in accordance with the assumptions given in Section 2. The list with the description of each case is presented in Table 2 and Table 3. The following denotations have been assumed in the tables in order to ease the identification of given case: A – narrow pane ($a/b > 2$), B – square pane ($a/b = 1$), L – linear support, P – point support, t – static analysis according to W–B, G–R–C, CEN computational

Table 2. List of cases – narrow panes

Case	Type of support	Way of support modelling	Solution
A1–L–t–20.76	linear support	–	analytical solution acc. CEN
A2–L–t–20.76	linear support	linear support (boundary condition)	effective thickness acc. W–B used in AxisVM, shell elements
A3–L–t–20.76	linear support	linear support (boundary condition)	effective thickness acc. G–R–C used in AxisVM, shell elements
A4–L–n–20.76	linear support	linear support (boundary condition)	exact geometry of glass pane, ABAQUS, solid elements
A5–P–t–20.76	pointwise support	–	analytical solution acc. CEN
A6–P–t–20.76	pointwise support	nodal support (boundary condition)	effective thickness acc. W–B used in AxisVM, shell elements
A7–P–t–20.76	pointwise support	nodal support (boundary condition)	effective thickness acc. G–R–C used in AxisVM, shell elements
A8–P–n–20.76	pointwise support	nodal support (boundary condition)	exact geometry of glass pane, ABAQUS, solid elements
A9–P–n–20.76	pointwise support	exact geometry, support modelled with solid elements	exact geometry of glass pane, ABAQUS, solid elements
A10–L–t–23.52	linear support	linear support (boundary condition)	analytical solution acc. CEN
A11–L–t–23.52	linear support	linear support (boundary condition)	effective thickness acc. W–B
A12–L–t–23.52	linear support	linear support (boundary condition)	effective thickness acc. G–R–C used in AxisVM, shell elements
A13–L–n–23.52	linear support	linear support (boundary condition)	exact geometry of glass pane, ABAQUS, solid elements
A14–P–t–23.52	pointwise support	–	analytical solution acc. CEN
A15–P–t–23.52	pointwise support	nodal support (boundary condition)	effective thickness acc. W–B
A16–P–t–23.52	pointwise support	nodal support (boundary condition)	effective thickness acc. G–R–C used in AxisVM, shell elements
A17–P–n–23.52	pointwise support	nodal support (boundary condition)	exact geometry of glass pane, ABAQUS, solid elements
A18–P–n–23.52	pointwise support	exact geometry, support modelled with solid elements	exact geometry of glass pane, ABAQUS, solid elements

Table 3. List of cases – square panes

Case	Type of support	Way of support modelling	Solution
B1–L–t–20.76	linear support	–	analytical solution acc. CEN
B2–L–t–20.76	linear support	linear support (boundary condition)	effective thickness acc. W–B used in AxisVM, shell elements
B3–L–t–20.76	linear support	linear support (boundary condition)	effective thickness acc. G–R–C used in AxisVM, shell elements
B4–L–n–20.76	linear support	linear support (boundary condition)	exact geometry of glass pane, ABAQUS, solid elements
B5–P–t–20.76	pointwise support	–	analytical solution acc. CEN
B6–P–t–20.76	pointwise support	nodal support (boundary condition)	effective thickness acc. W–B used in AxisVM, shell elements
B7–P–t–20.76	pointwise support	nodal support (boundary condition)	effective thickness acc. G–R–C used in AxisVM, shell elements
B8–P–n–20.76	pointwise support	nodal support (boundary condition)	exact geometry of glass pane, ABAQUS, solid elements
B9–P–n–20.76	pointwise support	exact geometry, support modelled with solid elements	exact geometry of glass pane, ABAQUS, solid elements
B10–L–t–23.52	linear support	–	analytical solution acc. CEN
B11–L–t–23.52	linear support	linear support (boundary condition)	effective thickness acc. W–B
B12–L–t–23.52	linear support	linear support (boundary condition)	effective thickness acc. G–R–C used in AxisVM, shell elements
B13–L–n–23.52	linear support	linear support (boundary condition)	exact geometry of glass pane, ABAQUS, solid elements
B14–P–t–23.52	pointwise support	–	analytical solution acc. CEN
B15–P–t–23.52	pointwise support	nodal support (boundary condition)	effective thickness acc. W–B
B16–P–t–23.52	pointwise support	nodal support (boundary condition)	effective thickness acc. G–R–C used in AxisVM, shell elements
B17–P–n–23.52	pointwise support	nodal support (boundary condition)	exact geometry of glass pane, ABAQUS, solid elements
B18–P–n–23.52	pointwise support	exact geometry, support modelled with solid elements	exact geometry of glass pane, ABAQUS, solid elements

procedures, n – static analysis using advanced computer modelling, 20.76 or 23.52 – total thickness of the glass pane. Thus the description B18–P–n–23.52 denotes 18^{th} consecutive glass pane 23.52 mm thick in total, with point support, for which the results have been obtained using advanced computer model.

The results of computer analyses are juxtaposed in Tables 4 through 11. It has to be noted, that the cases for which the results could not be obtained are listed in the tables as well. In those cases appropriate justification is given. For each considered glass pane a difference between listed result and the result obtained using the most advanced computer model in the series, expressed in percent, is given as well. The reference case in each series has been especially denoted.

Table 4. Maximum principal stresses and deflections – glass plate (0.35 × 1.5 m) simply supported along the edges, thickness 2 × 10 mm +0.76 mm

Case	σ_{max} [MPa] at midspan	w_{max} [mm]
A1–L–t–20.76	27.4 (−1.4%)	–[1]
A2–L–t–20.76	27.6 (−0.7%)	9.6 (−1.0%)
A3–L–t–20.76	27.7 (−0.4%)	9.7 (0.0%)
A4–L–n–20.76[2]	**27.8 (0.0%)**	**9.7 (0.0%)**

[1] The procedure for determining the deflections is not given [3, 7, 8]
[2] for this case the convergence test have been executed

Table 5. Maximum principal stresses and deflections – pointwise supported glass plate (0.35 × 1.5 m), thickness 2 × 10 mm +0.76 mm

Case	σ_{max} [MPa] at midspan	σ_{max} [MPa] in the support zone	w_{max} [mm]
A5–P–t–20.76	21.7 (+5.9%)	–	–[1]
A6–P–t–20.76	20.4 (−0.5%)	5.1 (−80.4%)	5.3 (−1.9%)
A7–P–t–20.76	21.3 (+3.9%)	5.7 (−78.1%)	5.7 (+5.6%)
A8–P–n–20.76	20.9 (+2.0%)	106 (+307.7%)	5.5 (+1.9%)
A9–P–n–20.76	**20.5 (0.0%)**	**26 (0.0%)**	**5.4 (0.0%)**

[1] Same as in Table 4

Sample results for selected plates are depicted in Fig. 2 through 6. Maximum principal stress distribution for case A8–P–n–20.76 is presented in Fig. 2. The rotule element for the following case A9–P–n–20.76 is depicted in Fig. 3. One should notice that relative glass displacements due to the interlayer deformation are clearly visible. Sample deflections for three layer square plate are given in Fig. 4. Finally, results presented in Fig. 2 should be analysed together with stress distribution obtained for precise support modelling (Fig. 5 and Fig. 6).

Table 6. Maximum principal stresses and deflections – glass plate simply supported along the edges, thickness 8 + 6 + 8 mm +2 × 0.76 mm

Case	σ_{max} [MPa] at midspan	w_{max} [mm]
A10–L–t–23.52	25.9 (−2.2%)	–[1]
A11–L–t–23.52	available only for a package of two layers of glass [15]	
A12–L–t–23.52	26.5 (+0.0%)	10.9 (0.0%)
A13–L–n–23.52	**26.5 (0.0%)**	**10.9 (0.0%)**

[1] Same as in Table 4

Table 7. Maximum principal stresses and deflections – pointwise supported glass plate (0.35 × 1.5 m), thickness 8 + 6 + 8 mm +2 × 0.76 mm

Case	σ_{max} [MPa] at midspan	σ_{max} [MPa] in the support zone	w_{max} [mm]
A14–P–t–23.52	21.3 (+0.9%)	–	–[1]
A15–P–t–23.52	available only for a package of two layers of glass [15]		
A16–P–t–23.52	20.5 (−2.8%)	5.1 (−63%)	6.5 (+6.6%)
A17–P–n–23.52	20.3 (−3.8%)	313 (+2168%)	6.3 (+3.3%)
A18–P–n–23.52	**21.1 (0.0%)**	**13.8 (0.0%)**	**6.1 (0.0%)**

[1] Same as in Table 4

Table 8. Maximum principal stresses and deflections – glass plate (1.5 × 1.5 m) simply supported along the edges, thickness 2 × 10 mm +0.76 mm

Case	σ_{max} [MPa] at midspan	w_{max} [mm]
B1–L–t–20.76	available only for simple bending [8]	
B2–L–t–20.76	10.3 (−14.9%)	2.9 (−21.6%)
B3–L–t–20.76	11.8 (−2.5%)	3.6 (−2.7%)
B4–L–n–20.76	**12.1 (0.0%)/13.6**[1]	**3.7 (0.0%)**

[1] local stresses at corners of the plate

Table 9. Maximum principal stresses and deflections – pointwise supported glass plate (1.5 × 1.5 m), thickness 2 × 10 mm +0.76 mm

Case	σ_{max} [MPa] at midspan	σ_{max} [MPa] in the support zone	w_{max} [mm]
B5–P–t–20.76	available only for simple bending [8]		
B6–P–t–20.76	23.0 (−3.0%)	25.5 (−49.3%)	9.9 (+2.1%)
B7–P–t–20.76	27.8 (+17.3%)	27.8 (−44.7%)	11.3 (+16.5%)
B8–P–n–20.76	25.4 (+7.2%)	1082 (+2051%)	11.0 (+13.4%)
B9–P–n–20.76	**23.7 (0.0%)**	**50.3 (0.0%)**	**9.7 (0.0%)**

Table 10. Maximum principal stresses and deflections – glass plate (1.5 × 1.5 m) simply supported along the edges, thickness 8 + 6 + 8 mm +2 × 0.76 mm

Case	σ_{max} [MPa] at midspan	w_{max} [mm]
B10–L–t–23.52	available only for simple bending [15]	
B11–L–t–23.52	available only for a package of two layers of glass [15]	
B12–L–t–23.52	12.1 (−0.8%)	4.5 (−2.2%)
B13–L–n–23.52	**12.2 (0.0%) / 14.4**[1]	**4.6 (0.0%)**

[1] local stresses at corners of the plate

Table 11. Maximum principal stresses and deflections – pointwise supported glass plate (1.5 × 1.5 m), thickness 8 + 6 + 8 mm +2 × 0.76 mm

Case	σ_{max} [MPa] at midspan	σ_{max} [MPa] in the support zone	w_{max} [mm]
B14–P–t–23.52	available only for simple bending [8]		
B15–P–t–23.52	available only for a package of two layers of glass [15]		
B16–P–t–23.52	31.5 (+10.1%)	29.0 (−46%)	13.8 (+22.1%)
B17–P–n–23.52	29.7 (+3.8%)	1345 (+2405%)	12.9 (+14.2%)
B18–P–n–23.52	**28.6 (0.0%)**	**53.7 (0.0%)**	**11.3 (0.0%)**

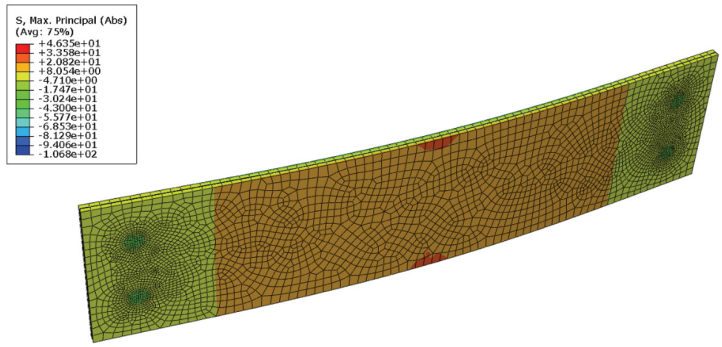

Fig. 2. Maximum principal stresses – A8–P–n–20.76

Additional computer models corresponding to cases B9–P–n–20.76 and B18–P–n–23.52 have been prepared to verify the applicability of the computational simplified approach presented in Section 2. The results obtained using the proposed method and results obtained with precise rendering of support geometry are compared in the Table 12. Moreover, appropriate graphic illustration is presented in Fig. 7. In the conducted simulations the openings in the glass pane have been expressly accounted for, therefore the factor described in [25] has not been applied.

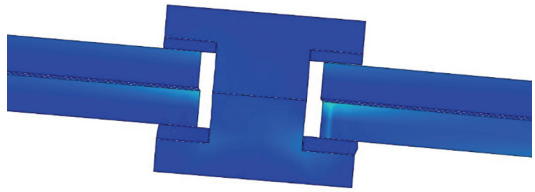

Fig. 3. Displacements, cross-section of the support – A9–P–n–20.76 (scale ×5, POM seal and finite element mesh are not visible)

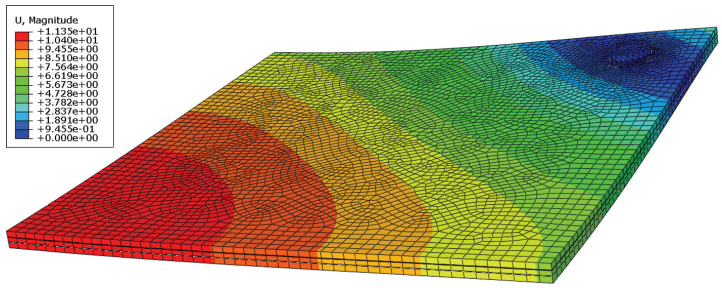

Fig. 4. Deflections – case B18–P–n–23.52 (results presented for a quarter of the plate)

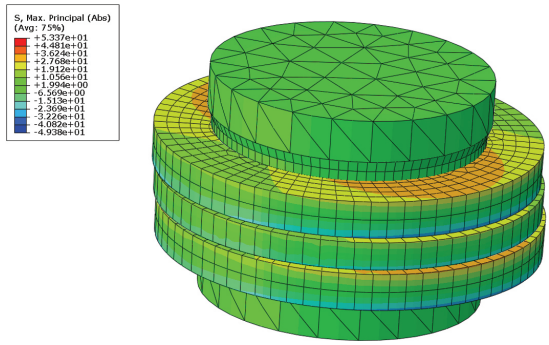

Fig. 5. Maximum principal stresses in the support zone – case B18–P–n–23.52

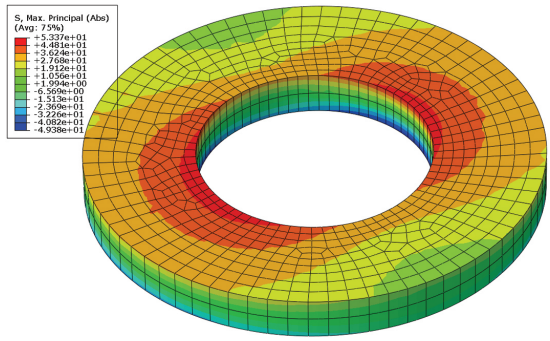

Fig. 6. The stress concentration around the hole in the glass plate – case B18–P–n–23.52

Table 12. Maximum principal stresses in the support zone – advanced and simplified approach

Case	Description	σ_{max} [MPa] in the support zone
B9–P–n–20.76	**exact geometry of the support, Table 9**	**50.3 (0.0%)**
B9–P–n–20.76-simplified	Abaqus, solid elements, simplified approach, stiffness of the support 17.5 MPa/mm	56.7 (+12.7%)
B9–P–n–20.76-simplified-2	Abaqus, solid elements, simplified approach, stiffness of the support 1.75 MPa/mm	33.2 (−34.0%)
B18–P–n–23.52	**exact geometry of the support, Table 11**	**53.7 (0.0%)**
B18–P–n–23.52-simplified	Abaqus, solid elements, simplified approach, stiffness of the support 17.5 MPa/mm	59.1 (+10.1%)
B18–P–n–23.52-simplified-2	Abaqus, solid elements, simplified approach, stiffness of the support 1.75 MPa/mm	**55.2** (+2.7%)

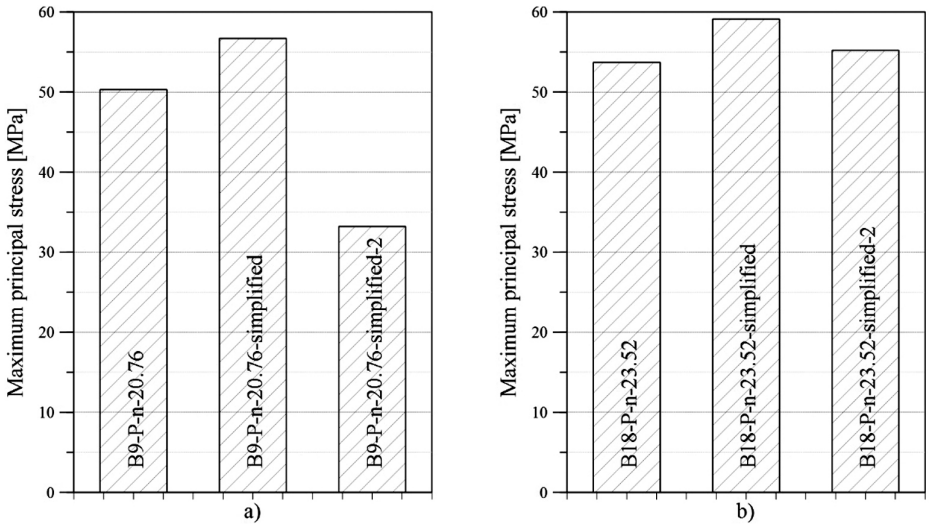

Fig. 7. The stress concentration around the hole in the glass plate – precise point support modelling versus simplified approach: a) B9–P–n–20.76, b) B18–P–n–23.52

4. Discussion of the results

All the analysed computational procedures (W–B, G–R–C, CEN) yielded satisfactory results regarding principal stresses in the span for narrow panes made of both two and three layer glass. The highest differences, reaching up to 6% with respect to the advanced computer model developed within the Abaqus environment, have been observed for CEN procedure (Table 5). Similar value has been obtained for W–B and G–R–C procedures with respect to the deflection magnitude. In such case the differences reached −1% (W–B, Table 4) and +6.6% (G–R–C, Table 7), respectively. However, the applicability of the W–B procedure is limited to panes comprising of two layers only. The results obtained for square panes are characterized by higher discrepancies. In the case of such elements W–B hypothesis may in certain cases yield significantly underestimated deflections (–21.6%, Table 8) as well as principal stresses in the span (–14.9%, Table 8). The G–R–C procedure in turn yields the results on the safe side, in almost every case overestimating the levels of both principal stresses (+10.1%, Table 11), and deflections. Taking into account the simplicity of application of the G–R–C method, one should consider the results obtained using this procedure as satisfactory. The justification for the differences between the results of advanced computer simulations and the results obtained using the G–R–C approach should be seen in the unavoidable limitations in accuracy of the tabular method applied to determine the coefficient ψ [15], not taking into account, among others, the detailed structure of the point support and its exact location with respect to the edge of glass pane.

Extremely high value of stresses in the support zone obtained for certain computer models (e.g. A8–P–n–20.76 and A17–P–n–23.52) require some additional explanation. Presented values have been estimated in the axis of the support. Therefore, they should be considered as a typical FEM singularities and they cannot be used for design purposes. Conversely, stresses calculated at a distance equal to the radius of the rotule are also unsatisfactory. They are definitely underestimated in each case (e.g. 3.7 MPa and 21.8 MPa for cases A8–P–n–20.76 and B8–P–n–20.76, respectively). Therefore, in order to calculate stress in the support zone advanced computer simulation is necessary. One has to note, that the practical application of the precise point support modelling, as presented in Sections 2 and 3, is difficult due to a number of unfavourable factors, such as the time consuming calculations or problems with convergence, which may be encountered during numerical analysis of a two body contact problem. The complexity level of the problem increases the risk of making errors at the geometry definition stage or while providing material data. Under such circumstances, as may be concluded based on data listed in the Table 12, the simplified mode of rendering an area support described in Section 2 may be considered a viable and effective computational approach. The results obtained using this approach are of sufficient accuracy for practical purposes. In addition these results depend only to a limited degree on the assumed stiffness. For the stiffness of 1.75 MPa/mm the results are underestimated in the case B9–P–n–20.76-simplified-2 by 34%, while for the stiffness of 17.5 MPa/mm the maximum differences remain within 12.7% (Table 12). It has to be remarked, that the applicability of simplified method presented in Section 2 is strictly limited to calculation of stresses in the support zone. This method under any circumstances

may not be applied to determine stresses or deflections in the span. Formulation of detailed guidelines regarding recommended stiffness of the area support requires further parametric analyses.

5. Conclusions

The results of the verification of selected computational procedures allowing to take into account the bonding effect of PVB foil in laminated glass panes are presented in this paper. The results of the analyses performed each time have been compared with the results of computer simulations varying in the level of complexity. Altogether 40 cases have been considered, encompassing narrow ($a/b > 2$) and square ($a/b = 1$) panes made of two or three layer glass.

The computational procedure based on the hypothesis presented by L. Galuppi and G. Royer-Carfagni should be considered the most universal. The remaining methods (CEN, W–B) may be applied only in limited scope. However, if the principal stresses in the zone adjacent to the support are sought, neither of the hypotheses considered here may be applied – an advanced computer model has to be used. The support itself may be modelled in an exact or simplified manner, conforming to the assumptions listed in Section 2.

References

[1] A. Piekarczuk, *Elementy konstrukcyjne ze szkła budowlanego*. Warszawa: Instytut Techniki Budowlanej, 2013.

[2] J. Belis, D. Mocibob, A. Luible, M. Vandebroek, "On the size and shape of initial out-of-plane curvatures in structural glass components", *Construction and Building Materials*, 2011, vol. 25, no. 5, pp. 2700–2712, DOI: 10.1016/j.conbuildmat.2010.12.021.

[3] K. Langosch, "Das Tragverhalten von Glasstützen mit Mono- und Verbundquerschnitten", PhD Dissertation, RWTH Aachen University, Germany, 2013.

[4] *DIN EN 13474-1. Glass in Building – Design of glass panes – Part 1: General basis of design*, 1999.

[5] *DIN EN 13474-2. Glass in Building – Design of glass panes – Part 2: Design for uniformly distributed loads*, 2000.

[6] M. Gwóźdź, *Konstrukcje szklane i aluminiowo szklane*. Kraków: Wydawnictwo Politechniki Krakowskiej, 2020.

[7] R. Kasper, K. Langosch, G. Siebert, *Guidance for European Structural Design of Glass Components support to the implementation, harmonization and further development of the Eurocodes*. Joint Research Centre, 2016, DOI: 10.2788/5523.

[8] M. Feldmann, R. Kasper, K. Langosch, *Glas für tragende Bauteile*. Berlin:Werner Verlag, 2012.

[9] M. Gwóźdź, "Formulae for buckling load bearing capacity of glass structure elements", *Archives of Civil Engineering*, 2020, vol. 66, no. 2, pp. 353–368, DOI: 10.24425/ace.2020.131814.

[10] G. Sedlacek, F. Wellershoff, H. Düster, *Bemessungsschubmodul für PVB Folien in Verbundsicherheitglas unter Klimatenlasten in Deutschland*. Bericht G 2003/10-06, RWTH Aachen, 2003.

[11] M. Gwóźdź, P. Woźniczka, "New static analysis methods for plates made of monolithic and laminated glass", *Archives of Civil Engineering*, 2020, vol. 66, no. 4, pp. 593–609, DOI: 10.24425/ace.2020.135239.

[12] Architectural Technical Applications Center, "Saflex®DG structural interlayer". [Online]. Available: www.mepla.net/media/medien/product-technical-sheet—saflex-dg_060415_9ab18.pdf. [Accessed: 20.12.2020].

[13] E. Wölfel, "Elastic Composite: An Approximation Solution and its Application Possibilities", *Stahlbau*, 1987, vol. 6, pp. 173–180.

[14] S.J. Bennison, L. Stelzer, "Structural properties of laminated glass. Short Course", presented at Glass Performance Days, 12–15 Jun. Tampere, 2009.

[15] National Research Council of Italy, *CNR-DT 210/2013. Guide for the Design, Construction and Control of Buildings with Structural Glass Elements*. Italy, 2013.

[16] L. Galuppi, G. Royer-Carfagni, "Effective thickness of laminated glass beams: New expression via variational approach", *Engineering Structures*, 2012, vol. 38, pp. 53–67, DOI: 10.1016/j.engstruct.2011.12.039.

[17] L. Galuppi, G. Royer-Carfagni, "The effective thickness of laminated glass plates", *Journal of Mechanics of Materials and Structures*, 2012, vol. 7, no. 4, pp. 375–400, DOI: 10.2140/jomms.2012.7.375.

[18] M. Asik, S. Tezcan, "A mathematical model for the behaviour of laminated glass beams", *Computers & Structures,* 2005, vol. 83, no. 21–22, pp. 1742–1753, DOI: 10.1016/j.compstruc.2005.02.020.

[19] P. Foraboschi, "Three-layered plate: Elasticity solution", *Composites Part B: Engineering*, 2014, vol. 60, pp. 764–776, DOI: 10.1016/j.compositesb.2013.06.037.

[20] P. Foraboschi, "Analytical model for laminated-glass plate", *Composites Part B: Engineering*, 2012, vol. 43, no. 5, pp. 2094–2106, DOI: 10.1016/j.compositesb.2012.03.010.

[21] J. Xu, Y. Li, B. Liu, M. Zhu, D. Ge, "Experimental study on mechanical behavior of PVB laminated glass under quasi-static and dynamic loadings", *Composites Part B: Engineering*, 2011, vol. 42, no. 2, pp. 302–308, DOI: 10.1016/j.compositesb.2010.10.009.

[22] Dassault Systemes Simulia Inc., *Abaqus Analysis User's Guide*. USA, 2010.

[23] B. Song, W. Chen, "One-Dimensional Dynamic Compressive Behavior of EPDM Rubber", *Journal of Engineering Materials and Technology*, 2003, vol. 125, no. 3, pp. 294–301, DOI: 10.1115/1.1584492.

[24] M. Cheng, W. Chen, "Experimental investigation of the stress-stretch behavior of EPDM rubber with loading rate effects", *International Journal of Solids and Structures*, 2003, vol. 40, no. 18, pp. 4749–4768, DOI: 10.1016/S0020-7683(03)00182-3.

[25] W.D. Pilkey, D.F. Pilkey, *Peterson's Stress Concentration Factors*, 3rd ed. New Jersey: John Wiley & Sons, 2008.

[26] B. Weller, M. Engelmann, F. Nicklisch, T. Weimar, *Glasbau-Praxis. Konstruktion und Bemessung. Band 2: Beispiele nach DIN 18008*, 3rd ed. Berlin – Vienna – Zurich: Beuth Verlag GmbH, 2013.

[27] J. Beyer, M. Seel, "Spannungsfaktoren für die Bemessung punktgestützter Verglasungen", *Stahlbau*, 2012, vol. 81, no. 9, pp. 719–727, DOI: 10.1002/stab.201201601.

[28] M. Tibolt, C. Odenbreit, "The stress peak at the borehole of point-fitted IGU with undercut anchors", *Journal of Facade Design and Engineering*, 2014, vol. 2, no. 1–2, pp. 33–66, DOI: 10.3233/FDE-130011.

[29] Inter-Cad Kft., *AxisVM X5 User's Manual*. Hungary, 2020.

[30] Dlubal Software GmbH, *RFEM 5. User Manual*. Germany, 2020.

[31] *DIN 18008-3. Glass in Building – Design and construction rules – Part 3: Point fixed glazing*. 2013, DOI: 10.31030/2006043.

[32] *DIN 18008-5. Glass in Building – Design and construction rules – Part 5: Additional requirements for walk-on glazing*. 2013, DOI: 10.31030/2006045.

Modelowanie komputerowe podpartych punktowo płyt ze szkła laminowanego

Słowa kluczowe: analiza nieliniowa, modelowanie komputerowe, podpora punktowa, szkło laminowane, teoria płyt cienkich

Streszczenie:

W ostatnich latach dokonano znaczącego postępu w zakresie konstrukcyjnego wykorzystania w budownictwie elementów ze szkła. Równocześnie trwają prace nad drugą edycją norm europejskich, wśród których przewidziano przygotowanie odrębnej normy dotyczącej projektowania konstrukcji szklanych. Zgodnie z dokumentami opracowanymi przez odpowiedni komitet techniczny Europejskiego Komitetu Normalizacyjnego, wspomniana norma powinna obejmować swoim zakresem także nowoczesne procedury w zakresie obliczeń statycznych prętów i płyt ze szkła laminowanego. Tego typu elementy konstrukcyjne podparte w sposób punktowy lub w sposób liniowy są powszechnie stosowane w praktyce inżynierskiej ze względów architektonicznych i funkcjonalnych. Problematyka związana z modelowaniem komputerowym elementów ze szkła, jak również procedury analityczne pozwalające na uwzględnienie zespalającego działania folii PVB, nie są jednak powszechnie znane i stosowane w środowisku inżynierskim. W tej sytuacji w artykule przedstawiono wyniki weryfikacji wybranych procedur obliczeniowych dotyczących płyt ze szkła laminowanego. W przeprowadzonych analizach uwzględniono metody obliczeniowe oparte na hipotezach opracowanych przez E. Wölfela i S.J. Bennisona, a także przez zespół autorski L. Galuppi i G. Royer-Carfagni. Rozpatrywano również ścisłe rozwiązanie zagadnienia zginanego pręta ze szkła laminowanego wyprowadzone z modeli reologicznych przez K. Langosch. Otrzymane rezultaty porównano każdorazowo z wynikami zaawansowanych symulacji komputerowych. W celu możliwie dokładnego odwzorowania zachowania się danej płyty szklanej oraz zespalającej warstwy PVB stosowano bryłowe elementy skończone, natomiast obliczenia były prowadzone jako geometrycznie nieliniowe. Szczególną uwagę poświęcono zagadnieniom związanym z analizą płyt podpartych w sposób punktowy. Naprężenia główne w strefie podporowej były wyznaczane dla modeli komputerowych o zróżnicowanym stopniu skomplikowania, w tym również dla przypadków w których uwzględniono dokładną geometrię danej rotuli. Omówiono propozycję uproszczonego sposobu modelowania strefy podporowej. Analizy były prowadzone dla dwóch grup płyt o zróżnicowanej geometrii. W zakresie rozwiązań poszczególnych płyt rozpatrywano elementy ze szkła dwu- oraz trójwarstwowego. W celach porównawczych w artykule przedstawiono również rezultaty uzyskane dla płyt podpartych w sposób przegubowo-liniowy. Na podstawie przeprowadzonych badań sformułowano wnioski w zakresie przydatności poszczególnych metod obliczeniowych.

Received: 21.12.2021, Revised: 25.01.2022